Applied Physics Letters ARTICLE scitation.org/journal/apl

An elementary photo-thermoelectric transistor: Experimental demonstration

Cite as: Appl. Phys. Lett. **116**, 243501 (2020); doi: 10.1063/5.0010264
Submitted: 8 April 2020 · Accepted: 31 May 2020 ·
Published Online: 15 June 2020

L. C. Rave-Osorio[1] and J. Alvarez-Quintana[1,2,a)]

AFFILIATIONS

[1]Centro de Investigación en Materiales Avanzados S. C. Unidad Monterrey, Alianza Norte # 202, Autopista Monterrey-Aeropuerto Km.10., C.P. 66628 Apodaca, Nuevo León, Mexico

[2]Genes-Group of Embedded Nanomaterials for Energy Scavenging, CIMAV-Unidad Monterrey, Alianza Norte # 202, Autopista Monterrey-Aeropuerto Km.10., C.P. 66628 Apodaca, Nuevo León, Mexico

[a)]Author to whom correspondence should be addressed: jaime.alvarez@cimav.edu.mx

ABSTRACT

Viable power supply methods capable of replacing the need for batteries are a key design factor for realization of emerging technologies and platforms based on self-sustainable standalone electronics. Hence, alternate possibilities should arise by developing semiconductor devices with an inherent energy source, i.e., a device that simultaneously exhibits energy-converting as well as amplifying-modulating properties. In the present Letter, we report a proof-of-concept photo-thermoelectric modulator. Thereby, an optical signal is reproduced by the thermoelectric voltage generated by modulating, with a light beam, the free carrier concentration of a photoconductive PbS film that is under a temperature gradient. Experimental results unveil that photo-generated electrons affect more electrical conductivity than thermal conductivity, giving rise to a drastic change in thermoelectric power. Consequently, it induces significant changes in the thermoelectric figure of merit of the device, and thus, signal modulation is mainly awarded to photo-generated electrons rather than thermal effects. Therefore, the device developed here establishes the basis for the development of an elementary batteryless photo-thermoelectric transistor and opens alternative avenues for self-powered devices that are driven by temperature gradients via a photo-thermoelectric effect.

Emerging platforms, such as Internet of Things (IoT),[1] Smart Skins (SSs),[2] and Smart Cities (SCs),[3] are networks of interconnected wireless sensors for a wealth of applications—all of which collect and share data about the environment around them with the aim of monitoring and detecting problem areas, without requiring human interaction. Evidently, such an interacting world will need to keep millions of sensors powered long term, and thereby, the major barrier to attain this is the battery. One solution is to make the devices self-powered, i.e., that power up themselves with energy harvested from their surroundings such as light, movement, heat, wind, and RF.[4] Nevertheless, current available solutions and components for energy harvesting on the market are complex and need different electronic systems to be functional in any operational condition. So it is not as simple as throwing out the battery and inserting an energy harvester. In this sense, any major distribution of batteryless and self-powered systems is something that still lies in the future. Hence, alternate possibilities should arise by developing semiconductor devices with an inherent energy source, i.e., a device that simultaneously exhibits energy-converting as well as amplifying-modulating properties. In this Letter, we report an elementary photo-thermoelectric modulator based on polycrystalline PbS films. The device is able to reproduce an optical signal into an electrical signal by means of a thermoelectric voltage generated by modulating, with a light beam, the free carrier concentration of a photoconductive PbS film that is under a temperature gradient. PbS was selected due to its exciting physical properties, which make it an excellent candidate in applications ranging from photodetection to solar photovoltaics.[5–9] Polycrystalline PbS films were prepared by the chemical bath deposition route as previously reported.[10] The aqueous bath of lead acetate-$Pb(NO_3)_2$, thiourea-$SC(NH_2)_2$, and sodium hydroxide-NaOH produced films of about 130, 270, and 450 nm thicknesses in 3, 4, and 6 h, respectively, onto ordinary glass slides. X-ray diffraction (XRD) studies show that these PbS films are nanocrystalline with crystallite sizes of 17, 19, and 24 nm. They exhibit a cubic phase, and the (hkl) planes are indexed using JCPDS data file No. 77–0244 with lattice constants of $a = b = c = 5.934$ Å, and $\alpha = \beta = \gamma = 90°$; Scanning Electron Microscopy (SEM) revealed that the films consist of stacked grains. Thermoelectric and photo-thermoelectric studies were carried out using a custom lab experimental setup, and the results show that

signal modulation is awarded to photo-generated electrons, which induces changes in the thermoelectric figure of merit due to a drastic change in thermoelectric power rather than the temperature dependence of thermoelectric properties. The concept of the proposed elementary photo-thermoelectric transistor is shown in the inset of Fig. 1(a). Basically, when a semiconductor slab is placed in between two heat reservoirs at different temperatures T_h and T_c, a thermovoltage $\Delta V_d = S_d(T_h - T_c)$ is induced. Here, S_d is the Seebeck coefficient, and it can be expressed as

$$S_d = \frac{k_B}{\sigma_d}\left[n\mu_n\left(2 - \frac{F}{k_B T}\right) - P\mu_p\left(2 + \frac{F + E_g}{k_B T}\right)\right]. \quad (1)$$

Clearly,

$$S_d \propto 1/\sigma_d,$$

where μ_n, μ_p, n, and p represent the mobility and content for electrons and holes, respectively. Besides, F and E_g stand for the Fermi level and gap energy, σ_d the electrical conductivity, and k_B the Boltzmann constant. Evidently, if the semiconductor slab is photoconductive, then under lighting, $\sigma_d \to \sigma_l$ due to the photo-generated electrons, and $S_l \propto 1/\sigma_l$. Thus, by altering the carrier concentration in the slab by means of photoelectric excitation, S_d is changed into S_l, and also, if the exciting light is modulated, then $S_l - S_d$ will follow this modulation, giving rise to a reproduced electrical signal where the output energy will come from the heat reservoirs. Figure 1(b) shows the proposed architecture for the device. It consists of a 450 nm thick PbS film deposited onto a slide of the glass substrate. Besides, Al contacts of 200 nm in thickness were patterned onto the PbS film surface by the conventional photolithography process.

Figure 1(c) presents an illustrative scheme of the experiment. The device is subjected to a steady state temperature gradient of 30 K above room temperature. Then, light pulses of 60 mW/cm^2 generated from a tungsten lamp are irradiated and thrown upon the device active area. Figure 1(d) shows the temperature rise detected between the sensors S_1 and S_2 due to light pulses; the increment is around 0.8 K. Simultaneously, the thermovoltage is logged; it can be seen in Fig. 1(e) that a steady state voltage at around −7.375 mV is present due to the temperature rise of 30 K. Nevertheless, such thermoelectric voltage is modulated by the photo-generated electrons via the light pulses, which induces a voltage drop of around 94 μV. Finally, thermoelectric voltage is contrasted directly with an arbitrary −7.4 mV dc signal using Labview signal comparison algorithms. Figure 1(f) shows the resulting logic pulse signal after comparison operation, and such a signal can be used either to control or as information signals. Hence, alternative possibilities toward the realization of batteryless modulating semiconductor devices should arise by using the property of semiconductors to change the thermoelectric power when the concentration of carriers (electrons and/or holes) is altered without changing the main temperature gradient.

For analytically understanding the operation and performance of the elementary thermoelectric modulator, we have examined the thermoelectric parameters of the PbS thin films under darkness and lighting. The inset in Fig. 2(a) shows the photoconductivity of the films as a function of their thickness, $\Delta\sigma(t) = \sigma_l - \sigma_d$ at room temperature. Clearly, as the thickness increases, photoconductivity increases; for this reason, the 450 nm film was used as a proof-of-concept device. That is, because of surface recombination, more charge carriers are lost at the surface in thinner samples than in thicker ones, and hence, the charge carriers reaching the bulk are less; thus, photoconductivity is reduced.[11] Figure 2(a) shows the temperature-dependent electrical conductivity of the 450 nm PbS film. By convention, we plot Ln(σ) vs the reciprocal temperature 1/T. From the plot, it can be deduced that PbS films show extrinsic conductivity under both lighting and darkness. At low enough temperatures, a change in the slope $\partial\sigma/\partial T$ from negative to positive is observed; such behavior is because in the depletion region, the majority carrier concentration remains practically constant, meaning that the heat applied is able to ionize the donors but not enough to ionize the electrons from the host lattice. The decrease in conductivity shows that the carrier density is not greatly influenced by temperature and the variations in mobility will determine the shape of the curve. At high enough temperatures, the conductivity is typically intrinsic. In this zone, the concentration of charge carriers generated by thermal excitation across the bandgap is now much larger; furthermore, as excitation occurs from the valence band to the conduction band, the hole concentration p = n. Hence, in an intrinsic semiconductor, the plot exhibits an Arrhenius behavior given by $\sigma(T) = \sigma_0 e^{-E_a/k_B T}$, where σ_0 is the pre-exponential factor, E_a is the activation energy, and k_B is the Boltzmann constant. It is clear

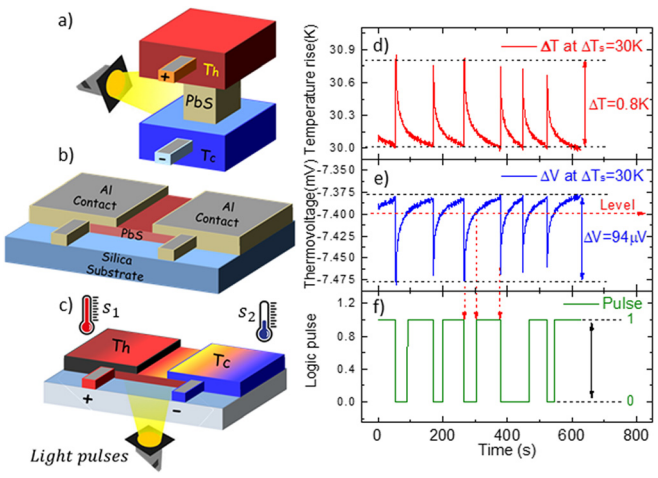

FIG. 1. (a) Device concept, (b) device architecture, (c) experimental setup, (d) temperature modulation, (e) thermovoltage modulation, and (f) logic pulse signal.

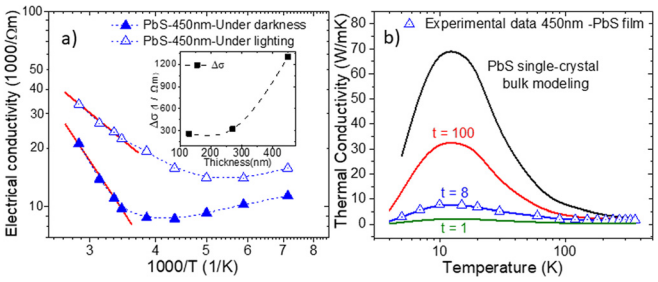

FIG. 2. Temperature dependence of (a) electrical conductivity and (b) thermal conductivity of the polycrystalline 450 nm PbS film.

that Ln(σ) linearly decreases with 1/T and the E_a values of the 450 nm-PbS film obtained from the best linear fits in the intrinsic region are 32.2 meV and 13.05 meV under darkness and lighting, respectively. As open triangle symbols, Fig. 2(b) shows the temperature-dependent thermal conductivity of the 450 nm-PbS film measured via the 3ω method.[12] To analyze further the experimental data in Fig. 2(b), we adopt a model for the thermal conductivity in polycrystalline materials based on the assumption of the phonon-hopping transport.[13] In this model, the conductivity within the grains follows bulk rules (single crystal thermal conductivity),[14] whereas the thermal resistance introduced by the grain boundaries is considered through the transparency parameter, t. A reasonable fitting to experimental data can be achieved with a fitting parameter of $t = 8$. Figure 2(b) also shows modeling for a high value of the transparency parameter, $t = 100$; this situation arises when the interface between adjacent grains almost does not exist; in this case, the thermal conductivity of the material tends to act as a bulk crystal. Conversely, if we assume a well-defined grain boundary, then the transparency parameter for the interface between adjacent grains takes lower values, i.e., $t = 1$, and the temperature dependence of the thermal conductivity of the material is closer to that of highly disordered microstructures. The reported k for bulk PbS is around 2.5 W/m K.[15,16] At room temperature, our experimental values for k are 1.76 W/m K, 0.82 W/m K, and 0.51 W/m K for the samples with 450, 270, and 130 nm, respectively. Likewise, the estimated value for a highly disordered PbS using the amorphous limit approach[17] is estimated to be 0.48 W/m K. Clearly, as the thickness increases, the sample tends to the bulk value, whereas thinner samples tend to accomplish the amorphous limit, which is reasonable taking into account that such samples present the lowest crystallite size, and therefore, they are greatly affected by the grain boundaries. Modeling calculations and experimental data of the full set of samples, as well as experimental details, are given in the supplementary material.

Focusing on the thermal and electrical conductivities of the 450 nm-PbS film in the vicinities of 300 K, which is the interest zone for modulator operation, we can observe in Fig. 3(a) that changes due to variations in temperature are 3.72×10^{-4} (W/m K)/K and 1.36×10^{3} (S/m)/K, respectively, whereas the change in electrical conductivity due to photoconductivity is $\Delta\sigma = 1.29 \times 10^{4}$ (S/m). Therefore, changes in electrical conductivity on account of photoconductivity are more significant that changes in the electrical and thermal conductivities due to variations in temperature. Thus, thermoelectric voltage shown in Fig. 1(e) is mainly modulated by the photo-generated

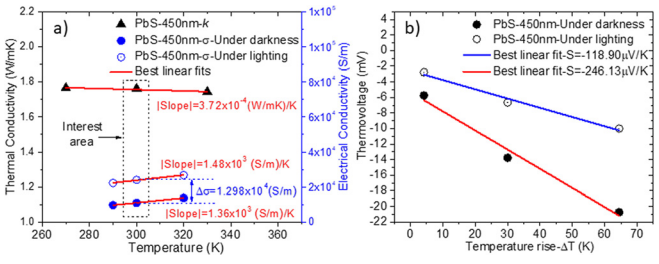

FIG. 3. (a) Thermal and electrical conductivities in the vicinities of 300 K and (b) Seebeck coefficient of the polycrystalline 450 nm PbS film under lighting and darkness.

TABLE I. Thermoelectric parameters of the 450 nm-PbS thin film.

Property	Darkness	Lighting	Reported
k (W/m K)	1.76	1.76	2.34
σ (S/m)	1.1×10^4	2.4×10^4	1.02×10^4
S (μV/K)	−246.13	−118.9	−240
ZT	0.114	0.058	0.075

carriers via the light pulses rather than possible heating effects induced by the light pulses. Likewise, Fig. 3(b) shows the characteristics ΔV–ΔT for the 450 nm-PbS film under darkness and lighting; from the corresponding slopes, the estimated Seebeck coefficients are −246.13 μV/K and −118.9 μV/K, respectively. Evidently, the decrement in the Seebeck coefficient under lighting is due to the improvement in the electrical conductivity because of photoconductivity.

Table I presents the thermoelectric parameters of the 450 nm-PbS thin film under lighting and darkness. It is worth mentioning that thermal conductivity remains the same for both conditions; the reason is that in PbS, the phonon contribution to the overall thermal conductivity is around 98.6%,[18] and thus, electron contribution is lower than phonon contribution. Besides, thermoelectric parameters shown in Table I match adequately those reported previously for p-Type PbS polycrystalline bulk samples under darkness.[19]

Based on those results, the thermoelectric figure of merit $ZT = S^2\sigma T/k$ has been estimated. Clearly, a significant decrement in ZT is observed, which is awarded to the reduction in the thermoelectric power of the material $S^2\sigma$ under lighting, which presumably leads to the reproduction of the optical signal into an electrical signal where the energy comes from the heat reservoirs.

In summary, we report an elementary photo-thermoelectric modulator based on polycrystalline PbS films. The device is able to reproduce an optical signal into an electrical signal by means of a thermoelectric voltage generated by modulating, with light pulses, the free carrier concentration of a photoconductive film that is under a temperature gradient. Signal modulation is awarded to photo-generated electrons, which induces changes in the thermoelectric figure of merit due to a drastic change in thermoelectric power rather than the temperature dependence of thermoelectric properties. Although the device developed here is only for proof-of-concept purposes, more sophisticated devices of potential interest might eventually be designed, i.e., by means of a combination of two photoconductive films of opposite conductivity types between common heat reservoirs; more thermoelectric voltage could be obtained. Therefore, the device developed here establishes the basis for a self-powered elementary photo-thermoelectric transistor, opening up alternative avenues for devices, which simultaneously exhibits energy-converting as well as amplifying-modulating properties that could be driven by temperature gradients.

See the supplementary material section for the deposition film method to get the PbS films, the morphological and structural information of the films through the XRD patterns and SEM analysis, as well as a description of the experimental methods and results for the thermal and electrical characterization of the whole set of samples. Likewise, a detailed modeling related to the influence of the

crystallinity and temperature on the behavior of thermal conductivity of the samples is presented.

This work was supported by the Mexican Council for Science and Technology-Conacyt Mexico, through the Grant for fundamental research under frame National Issues No.1358. L.C.R.O. thanks Conacyt Mexico for the fellowship.

DATA AVAILABILITY

The data that support the findings of this study are available within this article and its supplementary material.

REFERENCES

[1]M. Ammar, G. Russelo, and G. Crispo, J. Inf. Secur. Appl. **38**, 8–27 (2018).
[2]M. Shi, J. Zhang, H. Chen, M. Han, S. A. Shankaregowda, Z. Su, B. Meng, X. Cheng, and H. Zhang, ACS Nano **10**(4), 4083–4091 (2016).
[3]R. Novotný, R. Kuchta, and J. Kadlec, J. Telecommun. Syst. Manage. **3**(2), 1000117 (2014).
[4]M. Haras and T. Skotnicki, Nano Energy **54**, 461–476 (2018).
[5]H. D. Jahromi and M. Moaddeli, Mater. Res. Express **6**(11), 116220–116228 (2019).
[6]S. A. McDonald, G. Konstantatos, S. Zhang, P. W. Cyr, E. J. D. Klem, L. Levina, and E. H. Sargent, Nat. Mater. **4**, 138 (2005).
[7]K. W. Johnston, A. G. Pattantyus-Abraham, J. P. Clifford, S. H. Myrskog, D. D. Macweil, L. Levina, and E. H. Sagent, Appl. Phys. Lett. **92**, 151115 (2008).
[8]W. Shu Fen, G. Feng, and L. Mengkai, Langmuir **22**, 398 (2006).
[9]J. H. Warnes, N. Heckenberg, and H. Rubinsztein-Dunlop, Mater. Lett. **60**, 3332 (2006).
[10]P. K. Basu, T. K. Chaudhuri, K. C. Nandi, R. S. Saraswat, and H. N. Acharya, J. Mater. Sci. **25**, 4014–4017 (1990).
[11]S. Reynolds, M. Brinza, M. L. Benkhedir, and G. J. Adriaenssens, in *Springer Handbook of Electronic and Photonic Materials*, edited by S. Kasap and P. Capper, 2nd ed. (Springer Handbooks, 2017), Chap. 7, pp. 151–172.
[12]C. Dames, in *Annual Review of Heat Transfer* (Beggel House, Inc., 2013), Chap. 2, pp. 1–49.
[13]L. Braginsky, N. Lukzen, V. Shklover, and H. Hofmann, Phys. Rev. B. **66**, 134203 (2002).
[14]J. Callaway, Phys. Rev. **113**(4), 1046–1051 (1959).
[15]S. Johnsen, J. Q. He, J. Androulakis, V. P. Dravid, I. Todorov, D. Y. Chung, and M. G. Kanatzidis, J. Am. Chem. Soc. **133**, 3460–3470 (2011).
[16]L. D. Zhao, S. H. Lo, J. Q. He, H. Li, K. Biswas, J. Androulakis, C. Wu, T. P. Hogan, D. Y. Chung, V. P. Dravid, and M. G. Kanatzidis, J. Am. Chem. Soc. **133**, 20476–20487 (2011).
[17]D. G. Cahill, S. K. Watson, and R. O. Pohl, Phys. Rev. B. **46**(10), 6131–6140 (1992).
[18]A. A. El-Sharkawy, A. M. Abou EI-Azm, M. I. Kenawy, A. S. Hillal, and H. M. Abu-Basha, Int. J. Thermophys. **4**(3), 261–269 (1983).
[19]L. D. Zhao, J. He, S. Hao, C.-I. Wu, T. P. Hogan, C. Wolverton, V. P. Dravid, and M. G. Kanatzidis, J. Am. Chem. Soc. **134**, 16327–16336 (2012).